Volume 21, No 3 | International Journal of Radiation Research, July 2023

Dosimetric characteristics of tomotherapy and three-dimensional conformal radiotherapy for head and neck cancer

N. Monadi[1], D. Shahbazi-Gahrouei[1*], S. Monadi[2], L. Mahani[2], A. Shams[2], A. Akhavan[3], R. Mohammadi[4]

[1]Department of Medical Physics, School of Medicine, Isfahan University of Medical Sciences, Isfahan, Iran
[2]Department of Radiation Oncology, Seyed Al-Shohada Hospital, Isfahan University of Medical Sciences, Isfahan, Iran
[3]Assistant Professor of Radiation Oncology, School of Medicine, Isfahan University of Medical Sciences, Isfahan, Iran
[4]Department of Mathematics, Isfahan University of Technology, Isfahan, Iran

► ***Original article***

Corresponding author:
D. Shahbazi-Gahrouei, Ph.D.,
E-mail:
shahbazi@med.mui.ac.ir

Received: October 2022
Final revised: January 2023
Accepted: February 2023

Int. J. Radiat. Res., July 2023; 21(3): 427-434

DOI: 10.52547/ijrr.21.3.11

Keywords: *Head and Neck Cancer, Conformity index; Homogeneity index; Radiotherapy, Three-Dimensional Conformal Radiation Therapy, Helical Tomotherapy.*

ABSTRACT

Background*:** This study aims to evaluate and compare Three-Dimensional Conformal Radiotherapy (3D-CRT) versus Helical Tomotherapy (HT) based on treatment planning and selection of the most appropriate method to reduce side effects. ***Materials and Methods: Treatment planning was performed on images of 20 patients with head and neck cancer with lymph node involvement by HT and 3D-CRT techniques in Seyed Al-Shohada hospital, Isfahan, Iran. The quality of target coverage, the exposure of normal tissue, and radiation delivery efficiency in two studied methods were compared. ***Results*:** Tomotherapy showed significant improvement over 3D-CRT in terms of D2%, D50% Dmean, V95%, CI (conformity index), and HI (homogeneity index) for PTV (planning target volume) and in terms of D2%, D98%, Dmean, V95%, CI and HI for PTV Nodal. The mean dose received by 98% of PTV (D98%) increased in HT compared to 3D-CRT. Whereas, higher doses received in organs at risk (OARs) in 3D-CRT compared to HT. ***Conclusion*:** Results showed improvements in target quality for HT over 3D-CRT, including dosimetric coverage of target volumes, homogeneity and conformity indices, and reduction of the volume of cold and hot spots. Tomotherapy also performed better than that of 3D-CRT in OARs. Overall, with the satisfactory results obtained here, HT technique has considerable promise for treating head and neck cancers with the involvement of regional lymph nodes.

INTRODUCTION

Head and neck cancers (HNC) occur in the mouth, lips, nose, sinuses, larynx, salivary glands, and throat [(1)]. These cancers remain a significant problem due to their high morbidity and mortality. The spread of these cancers is often through the lymph nodes in the neck. Head and neck cancer are often malignant and, therefore in most cases, require regional lymph nodes treatment. One of the main treatment methods for this type of cancer is radiation therapy.

Head and neck cancer is a technically challenging treatment site in radiation oncology due to the complex anatomy and numerous organs at risk (OARs) near targets [(2)]. These sensitive volumes include the right parotid, left parotid, mandible, oral cavity, thyroid, constrictor, right lens, left lens, brainstem, optic chiasm, right optic nerve, left optic nerve, right cochlea, left cochlea, cervical esophagus, tongue, larynx, right lung, left lung and spinal cord. Each of these organs has a different tolerance dose, and therefore the dose distribution in this region is crucial [(3)].

Radiation therapy usually leads to complications in the short or long term. These include salivary gland dysfunction, xerostomia, inflammation of the oral mucosa, the concentration of saliva, sore throat, earache, trismus, weight loss, taste dysfunction (dysgeusia), and dysphagia [(4)]. Depending on the region of the malignancy, these complications may occur early or late after starting treatment. To reduce these complications as much as possible and improve patients' quality of life after treatment, the protection of these sensitive volumes is critical and necessary.

Radiotherapy treatment planning aims to provide the best dose conformation to the target volume while sparing critical organs and healthy tissues [(5)]. Over the past decades, significant advances in radiotherapy techniques have been made to improve the quality of treatment and significantly reduce the side effects of this type of treatment. These advances in conformal radiotherapy first came in 3D-CRT

[DOI: 10.61186/ijrr.21.3.427]

(three-dimensional conformal radiotherapy) and then IMRT (intensity-modulated radiotherapy). Both 3D-CRT and IMRT represent a significant advance over conventional radiotherapy because they increase dose delivery accuracy while sparing surrounding normal tissues and OARs. Three-dimensional radiotherapy indicates the radiation transfer into a 3D volume using appropriate imaging and computer software [6]. Intensity-modulated radiotherapy is an advanced method for delivering three-dimensional therapy using radiation that delivers the maximum dose to the tumor and the minimum dose due to unwanted radiation to critical structures [7]. Also, the intensity of each beam is controlled, and the shape of the beam changes during the treatment [8]. Hence, it delivers a conformal dose to tumors and OARs while sparing them from damage by dropping the dose gradient in OARs [9]. The dose-modulating ability of IMRT gives a theoretical advantage over 3D-CRT, which recently has also been supported in the clinical trial [10, 11].

Helical tomotherapy is an IMRT method in which the patient is treated with a slice-by-slice CT scan by IMRT. A special collimator is designed for it, the gantry rotates around the patient's longitudinal axis, and the couch moves continuously as in the helical CT method [12, 13]. Tomotherapy delivers IMRT treatment with 64 pneumatically driven leaves of MLC, selectable fixed jaws, and 360° gantry rotation while the couch is translating [14]. The HT delivery of IMRT allows excellent conformity and homogeneity of the radiation dose distribution [15-19]. The advantage of this technique to radiation delivery seems to be suitable and effective, especially for complicated dose distributions involving multiple planning target volumes (PTVs) and organs at risk (OARs). Tomotherapy is often required for adequate and safe treatment of head and neck cancer [16]. Head and neck cancers are indications for advanced radiation therapy. Due to the lack of advanced facilities and treatment methods such as IGRT (image-guided radiotherapy), VMAT (volumetric modulated arc therapy), IMRT, and HT in developing countries such as Iran, radiotherapy for head and neck cancers is still performed by 3D-CRT. However, the 3D-CRT method cannot protect the OARs in this region and maintain their function, so using new techniques to reduce complications and improve the patient's quality of life is vital.

The current method (3D-CRT) has some limitations. For example, limitations in delivering adequate doses to target volumes while focusing on the sparing OARs and the impossibility of sparing adjacent normal tissues when delivering the required dose to target volumes [20].

Tomotherapy is a relatively new technique, and although it is superior to 3D-CRT in terms of tumor dose coverage, there are still some concerns about doses in OARs. Due to the installation and the implementation of this method in the radiotherapy department of Syed Al-shohada in Isfahan, its investigation of dose delivery in different target volumes and OARs is very important. This study aimed to prove the quality of treatment with HT versus 3D-CRT and to evaluate and compare based on treatment planning and selection of the most appropriate method to reduce side effects.

MATERIALS AND METHODS

Patient selection

In this study, CT images of 20 patients with malignant tumors of the head and neck, were considered in the radiotherapy department of Seyed Al-shohada Hospital, Isfahan, Iran. Patients with a history of radiotherapy were not included in this study. Prescription dose and the number of treatment sessions based on the type of treatment (curative or palliative), location, and type of malignancy were assessed. In each treatment session, the standard dose between 180 to 220 cGy was used for therapeutic goals. The dose was 50-74 Gy and 50-60 Gy for primary purposes and regional lymph nodes, respectively. More details of tumor location and prescribed doses are presented in table 1.

In Tomotherapy, the treatment planning was SIB (simultaneous integrated boost). But, in 3D-CRT plans, after the first phase, the treatment plans were changed and the next phases (boost) were planned by cord sparing approach and according to the different dose prescriptions of the lymph nodes and primary target as mentioned in table 1. Finally, the main plan and the boost plan were merged and the data was extracted from the merged plan.

For nasopharynx, hypopharynx, and oral cavity tumors, the prescription dose for PTV and PTV LN (lymph nodes) were 70 and 54/60 Gy, respectively. For mandible and base of tongue (BOT) malignancy, the prescription dose for PTV and PTV LNs was 60 and 54 Gy, respectively. The prescription dose for laryngeal cancer was 66 and 54 Gy for PTV and PTV LNs, respectively.

Data collection

To collect the patient data several steps including; multiple imaging, patient fixation and immobilization for treatment repeatability, image fuse, delineation of target volume structures and OARs, treatment planning, and evaluation of treatment plans were performed.

In this study, a special type of CT scan called CT simulation is used. CT simulation was performed using 20 slices (Siemens, SOMATOM) with thicknesses of 2 mm in the range of the head to the supernatural. To improve the detection of target volumes and OARs, MR and PET images were obtained and fused with CT images. For better

[DOI: 10.61186/ijrr.21.3.427]

conformity, all MR and PET image criteria were the same as CT conditions including slice thickness, the field of view (FOV), and positioning.

Table 1. Details of tumor site and prescription doses for each patient.

Patient	Tumor Site	Prescription (Gy) Primary/Lymph Node
1	Hypopharynx & LN	70/54
2	BOT & LN	60/54
3	Nasopharynx & LN	70/60
4	Nasopharynx & LN	70/60
5	BOT & LN	60/54
6	Larynx & LN	66/60
7	Nasopharynx & LN	70/54
8	Larynx & LN	60-70/54
9	Larynx & LN	74/60
10	Mandible & LN	60/54
11	BOT & LN	63/50.40
12	Nasopharynx & LN	50/50
13	Oral Cavity (Buccal) & LN	70/54
14	Nasopharynx & LN	70/60R-LN&54L-LN
15	Oropharynx & LN	66/60
16	Nasopharynx & LN	70/59.4
17	Larynx & LN	60-70/54
18	Hypopharynx, Larynx & LN	70/54R-LN&60L-LN
19	Nasopharynx & LN	70/54R-LN&60L-LN
20	Oral Cavity & LN	60/54

The radiation oncologist delineates all target volumes and OARs infused images based on ICRU 50, 62, and 83 protocols. Adjacent critical structures include the oral cavity, mandible, right parotid, left parotid, optic chiasm, right optic nerve, left optic nerve, right lens, left lens, brainstem, constrictor, right cochlea, left cochlea, larynx, thyroid, right lung, left lung, and spinal cord.

The TiGRT treatment planning system was performed based on Full Scatter Convolution (FSC) algorithm in 3D-CRT and PRECISION based on Collapsed Cone Convolution Superposition (CCCS) algorithm in HT.

Dose constraints of target volumes and OARs

Treatment planning and plan optimization should be done in a way that, according to ICRU62 and ICRU83, more than 95% of the prescribed dose reaches 95% of the volume of PTV. Ideally, the target volume dose should be kept at more than 95% and less than 107% of the prescribed dose. At the same time, the dose of all adjacent critical structures should be kept below their tolerance dose. Dose constraints of the OARs are given in table 2.

Treatment planning evaluation

According to ICRU 50, 62, and 83 reports, 3D-CRT and HT treatment planning evaluations are based on DVH (dose-volume histogram) the information obtained from patients' dose distributions in the treatment planning system.

Percentage of target volume receiving 95% of the prescribed dose ($V_{95\%}$), mean dose (D_{mean}), and dose received by 98% ($D_{98\%}$), 2% ($D_{2\%}$), and 50% ($D_{50\%}$). Also, CI and HI indices were extracted for the PTV in HT and 3D-CRT methods using DVH information. Both HI and CI indices were determined using the following equations:

$$HI = D_{2\%} - D_{98\%} / D_{50\%} \quad (1)$$

where $D_{2\%}$, $D_{98\%}$ and $D_{50\%}$ are the doses received by 2%, 98% and 95% of PTV volume, respectively.

$$CI = V_{RI} / TV = \text{reference isodose volume} / \text{target volume} \quad (2)$$

The ratio of the volume received by the reference isodose to the target volume, in which the volume of isodose is 95%, or in other words, the volume that received 95% of the prescribed dose is considered as the reference volume of PTV.

Table 2. Dose constraints of OARs.

Organ	Dose constraint	Reference
Optic Nerve	$D_{max} < 54$ Gy $D_{1CC} < 55$ Gy $D_{mean} < 50$ Gy	RTOG 0619
Optic chiasm	$D_{max} < 54$ Gy $D_{1CC} < 55$ Gy $D_{mean} < 50$ Gy	RTOG 0619
Lens	$D_{max} < 25$ Gy	RTOG 0615
Brainstem	$D_{max} < 54$ Gy $D_{1\text{-}10cc} < 59$ Gy	RTOG 0615 (30, 31)
Cochlea	$D_{mean} < 35$ or 45 Gy $V_{55} < 5\%$	(30) RTOG 0615
Oral cavity	$D_{max} < 60$ Gy $D_{mean} < 35$ or 40 Gy	RTOG 1016 RTOG 1016-0615
Mandible	$D_{max} < 66$ or 70 Gy $V_{1cc} < 75$ Gy $V_{75} < 1\%$	RTOG 1016-0615,(30) RTOG 0615
Larynx	$D_{mean} < 45$ Gy $V_{50} < 27\%$	(31,30)
Thyroid	$D_{max} < 50$ Gy $V_{45} < 45$ Gy	By clinics
Spinal cord	$D_{max} < 45$ or 50 Gy $D_{max} < 48$ Gy	RTOG 0615, (30, 31) RTOG 1016
Constrictor	$D_{mean} < 30$-50 Gy $D_{max} < 60$ Gy	(31, 30)
Parotid	$D_{mean} < 26$ Gy	RTOG 0619-0522-1016
Lung	$V_{20} < 30\%$ $V_5 < 42\%$	(31 ,30)

Abbreviations: D2%: dose covering 2% of PTV, D50%: dose covering 50% of PTV; D95%: dose covering 95% of PTV; D98%: dose covering 98% of PTV; Dmax: maximum dose; Dmean: mean dose; D1cc: dose covering 1 cm3 of PTV, Percentage of V5, V20, V45, V50, V55, V75: represent volumes of 5, 20, 50, 55, and 75 of PTV. *Statistically significant at the level of 5%.

OARs evaluation

In table 2, D_{max} is reported for serial organs such as right and left optic nerve, optic chiasm, and spinal cord. Also, in this table, the dose constraint is obtained for parallel organs like the parotid. Sometimes, the target volumes overlap occurs with critical structures.

Statistical analysis

To compare the means of the two methods, the Wilcoxon signed ranks test was used. A non-parametric test used to analyze two sets of data

[DOI: 10.61186/ijrr.21.3.427]

obtained from the same individuals, especially when there is an extreme violation of the normality assumption. This test is available in the SPSS statistical software (SPSS, Chicago, IL, USA). The null hypothesis for this test is that the medians of the two samples are equal. A P-value smaller than 0.05 is considered statistically significant.

RESULTS

Tomotherapy and 3D-CRT treatment planning methods were done on the images of 20 patients according to the tumor location, the prescribed dose of PTV 95%, and the dose constraints of OARs which are reported in table 2. Based on these conditions, an example of dose distribution around therapeutic targets for one of the patients is shown in axial, sagittal, and coronal views (figure 1). In addition, a more accurate dose distribution is identified using the same patient's DVH curve in two studied methods (figure 2).

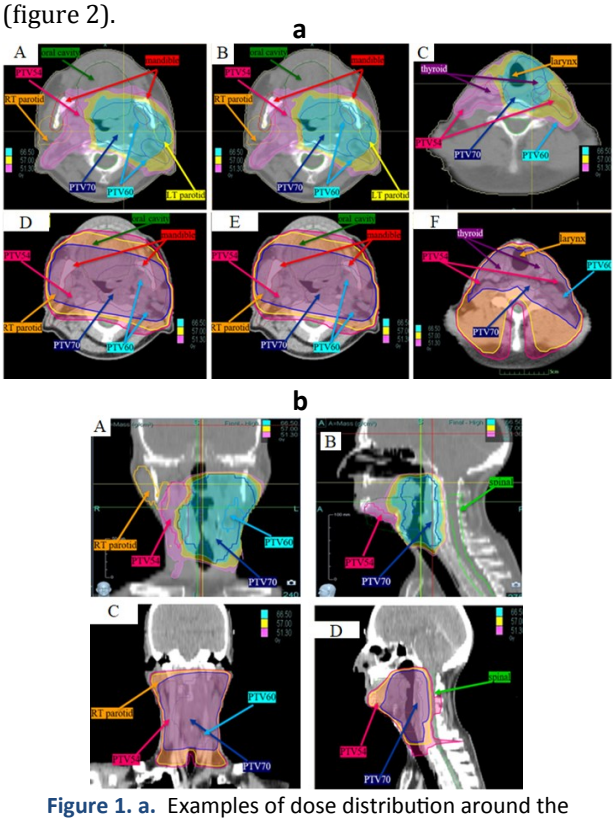

Figure 1. a. Examples of dose distribution around the therapeutic target organs with different PTV of a patient with head and neck cancer using HT **(A, B, C)** and 3D-CRT **(D, E, F)** methods in axial view; **b)** for the same patient using HT in coronal **(A)** and in sagittal **B)** views, using 3D-CRT in coronal **(C)** and in sagittal **(D)** views.

Primary PTV

For evaluation of primary PTV, the parameters ($D_{2\%}$, $D_{98\%}$, $D_{50\%}$, D_{mean} $V_{95\%}$, CI, and HI) were extracted in 3D-CRT and HT using DVH data, and the mean results of the two methods are compared (Table 3). As Table 3 shows, the mean dose received by 98% of PTV ($D_{98\%}$) increased in HT but, did not show a significant difference. The mean dose received by 2% of PTV ($D_{2\%}$) was found to be 72.60±5.88 and 68.43±5.88, in 3D-CRT and HT, respectively, which is a significant difference (P=0.000). Increasing the dose close to the minimum or $D_{98\%}$ and decreasing the dose close to the maximum or $D_{2\%}$ in the HT means reducing the hot and cold spots. Mean values of D_{mean} and $D_{50\%}$ also show significant differences between the two studied methods (P=0.000 and 0.007, respectively). The PTV that receives 95% of the prescribed dose ($V_{95\%}$) shows a significant increase in the HT method compared to 3D-Cindicatingcate better dosimetric coverage of target volume in HT.

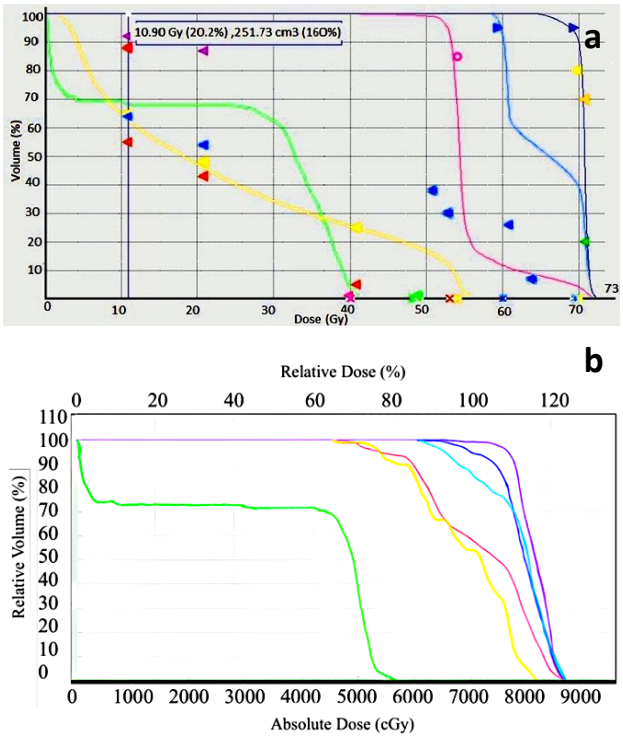

Figure 2. Examples of a dose-volume histogram (DVH) for head and neck cancer patient in; a) HT and b) 3D-CRT plans. Note*: Red (PTVLN54), Green (spinal cord), Yellow (right parotid), Blue (PTVLN60), Navy blue (PTV), and Purple (GTV).

Table 3. Evaluation parameters of primary PTV dose coverage in 3D-CRT and HT.

Parameter	HT ($\bar{X}$±S)	3D-CRT ($\bar{X}$±S)	P-value
$D_{98\%}$ (Gy)	63.29±5.31	63.21±5.86	0.852
$D_{2\%}$ (Gy)	68.43±5.88	72.60±7.38	0.000*
D_{mean} (Gy)	66.12±5.47	68.75±6.69	0.000*
$V_{95\%}$ (%)	99.54±0.74	95.71±6.99	0.020*
$D_{50\%}$ (Gy)	66.57±5.47	68.24±6.29	0.007*

Abbreviations: D2%: dose covering 2% of PTV, representing the near maximal dose; D50%: dose covering 50% of PTV; D95%: dose covering 95% of PTV; D98%: dose covering 98% of PTV; Dmean: mean dose. *Statistically significant at the level of 5%. Errors are standard deviation; the last column shows the P-value between the two groups. * is a sign that the difference between the two groups is significant.

The result calculations of CI and HI indices according to the equations (1 and 2) are presented in table 4. The mean CI for 3D-CRT and HT was significantly different with values of 0.25±0.15 and 1.36±0.26, respectively (P=0.000), which indicates better conformance of PTV to the prescription

[DOI: 10.61186/ijrr.21.3.427]

isodose curve in HT compared to 3D-CRT. The average HI is equal to 0.14±0.05 and 0.07±0.03 in HT and 3D-CRT, respectively and showed a significant decrease in HT (P=0.001).

Table 4. PTV conformity and homogeneity indices in 3D-CRT and HT.

parameter	HT ($\bar{X}$±S)	3D-CRT ($\bar{X}$±S)	P-value
CI	1.36±0.26	0.25±0.15	0.000*
HI	0.07±0.03	0.14±0.05	*0.001

Abbreviations: HI: Homogeneity index; CI: Conformity index. *Statistically significant at the level of 5%. Errors are standard deviation; the last column shows the P-value between the two groups. *: is a sign that the difference between the two groups is significant.

Nodal PTV

For nodal PTV, the same as primary PTV all extracted parameters are given in table 5. Comparison of $D_{2\%}$ (P=0.000), $D_{98\%}$ (P=0.007), D_{mean} (P=0.001), $V_{95\%}$ (P=0.000), CI (P=0.000), and HI (P=0.000) for 3D-CRT and HT showed significant differences, indicating better dose delivery and coverage of the HT than 3D-CRT.

Table 5. Evaluation parameters of Nodal PTV dose coverage in 3D-CRT and HT.

Parameter	HT ($\bar{X}$±S)	3D-CRT ($\bar{X}$±S)	P-value
$D_{98\%}$ (Gy)	52.78±3.51	49.66±4.73	0.007*
$D_{2\%}$ (Gy)	63.61±6.14	68.84±7.36	0.000*
D_{mean} (Gy)	57.39±3.33	59.74±4.86	0.001*
$V_{95\%}$ (%)	98.13±1.48	80.05±20.54	0.000*
$D_{50\%}$ (Gy)	56.53±3.54	56.18±14.44	0.070

Abbreviations: D2%: dose covering 2% of PTV, representing the near maximal dose; D50%: dose covering 50% of PTV; D95%: dose covering 95% of PTV; D98%: dose covering 98% of PTV; Dmean: mean dose. *Statistically significant at the level of 5%. Errors are standard deviation; the last column shows the P-value between the two groups. * is a sign that the difference between the two groups is significant.

Table 6. Nodal PTV conformity and homogeneity indices in 3D-CRT and HT.

Parameter	HT ($\bar{X}$±S)	3D-CRT ($\bar{X}$±S)	P-value
CI	1.31±0.25	0.06±0.08	0.000*
HI	0.17±0.08	0.34±0.11	0.000*

Abbreviations: HI: Homogeneity index; CI: Conformity index. *Statistically significant at the level of 5%. Errors are standard deviation; the last column shows the P-value between the two groups. *: is a sign that the difference between the two groups is significant.

Dose received by OARs in 3D-CRT and HT

A dose comparison of the OARs includes the brainstem, cochlea, constrictor, larynx, lenses, lungs, mandible, optic chiasm, optic nerves, oral cavity, parotids, spinal cord, and thyroid is given in table 7.

For serial structures such as the brainstem, spinal cord, optic chiasm, optic nerves, and lenses, it is necessary to focus on the D_{max} when evaluating. It is better to concentrate on the mean dose values for evaluating parallel structures such as the mandible, larynx, and cochlea (D_{mean}).

According to data in table 7, In HT compared to 3D-CRT, the maximum dose received for brainstem, D_{1cc}, and D_{10cc}, respectively and decreased by 14, 17.39, and 10.18 Gy, which are significant differences (P=0.001, P=0.001, and P=0.001). The mean dose (D_{mean}), V_{55}, and D_{max} were measured for right and left cochlea. The values of all three parameters were reduced in the HT method compared to 3D-CRT, and D_{mean} showed a significant difference for right and left cochlea (P = 0.028, P=0.047), respectively. The decrease in D_{max} was significant only for left cochlea (P=0.037), and V_{55} did not show a significant difference despite the reduction in volume percentage. The D_{mean} and D_{max} values were considered for constrictors, which significantly reduced the HT technique (P <0.05). Mean dose (D_{mean}), D_{max}, and V_{50} values for larynx and optic chiasm, right and left optic nerves, and oral cavity was extracted from treatment plans, all of which had a significant reduction in HT compared to 3D-CRT. The D_{max} values of the right lens, V_{20} for the right and left lungs, D_{max} and D_{1cc} for the mandible, and V_{45} for the thyroid were significantly decreased for the HT (P <0.05). D_{mean} for right and left parotids and D_{max} for the spinal cord was measured and a reduction of 26.99 Gy for the D_{mean} of right parotid (P=0.002) and 30.66 Gy for the D_{mean} of left parotid (P=0.000) and 12.51 for the D_{max} of the spinal cord (P=0.000) are important and remarkable advantages of HT over 3D-CRT. For the other parameters, a decrease in values was observed in the HT method, but the P values did not show a significant difference.

Table 7. Comparison of dose received by OARs of head and neck in 3D-CRT and HT.

Organ	Parameter	HT ($\bar{X}$±S)	3D-CRT ($\bar{X}$±S)	P-value
Brainstem	D_{max} (Gy)	32.09±16.40	46.09±18.16	0.001*
	D_{1cc} (Gy)	24.06±17.21	41.45±20.21	0.001*
	D_{10cc} (Gy)	9.50±11.76	19.68±21.20	0.001*
Right Cochlea	D_{mean} (Gy)	23.23±18.67	32.12±29.65	0.047*
	V_{55} (%)	10.55±27.93	37.73±49.74	0.180
	D_{max} (Gy)	26.32±23.14	34.12±30.18	0.059
Left Cochlea	D_{mean} (Gy)	19.58±13.16	31.62±27.18	0.028*
	V_{55} (%)	0.00±0.00	27.18±42.66	0.180
	D_{max} (Gy)	25.13±17.06	35.19±30.02	0.037*
Constrictor	D_{mean} (Gy)	44.07±8.84	58.80±5.69	0.003*
	D_{max} (Gy)	66.32±6.18	70.03±5.11	0.016*
Larynx	D_{mean} (Gy)	35.57±17.82	57.29±7.48	0.000*
	D_{max} (Gy)	56.16±9.77	64.58±11.83	0.002*
	V_{50} (%)	21.90±38.20	77.77±22.25	0.001*
Right Lens	D_{max} (Gy)	5.80±15.46	8.24±17.59	0.016*
Left Lens	D_{max} (Gy)	5.83±15.42	6.60±16.81	0.320
Right lung	V_{20} (%)	11.09±6.62	13.54±10.94	0.005*
	V_5 (%)	22.77±14.65	19.07±14.58	0.388
	D_{mean} (Gy)	7.78±4.55	7.73±5.66	0.084
Left Lung	V_{20} (%)	10.92±6.86	13.33±9.81	0.008*
	V_5 (%)	23.37±15.41	19.40±14.79	0.695
	D_{mean} (Gy)	7.72±4.90	7.69±5.28	0.077
Mandible	D_{max} (Gy)	62.50±9.56	70.14±6.83	0.000*
	D_{1cc} (Gy)	58.81±10.87	68.96±6.74	0.000*
	V_{75} (%)	0.00±0.00	1.60±5.64	0.068
Optic chiasm	D_{max} (Gy)	6.34±11.23	14.45±23.41	0.001*
	D_{mean} (Gy)	5.36±9.84	13.46±22.40	0.006*
Right Optic nerve	D_{max} (Gy)	11.60±21.22	16.77±25.28	0.006*
	D_{mean} (Gy)	8.27±16.72	13.58±21.71	0.004*
Left Optic nerve	D_{max} (Gy)	8.80±14.81	15.86±24.34	0.001*
	D_{mean} (Gy)	5.97±10.37	12.72±20.80	0.013*
Oral Cavity	D_{max} (Gy)	66.86±8.41	71.61±6.05	0.001*
	D_{mean} (Gy)	41.08±7.02	50.18±14.55	0.020*
Right Parotid	D_{mean} (Gy)	25.33±10.76	52.32±12.68	0.002*
Left Parotid	D_{mean} (Gy)	25.92±11.62	56.58±9.01	0.000*
Spinal cord	D_{max} (Gy)	40.50±4.69	53.01±2.67	0.000*
Thyroid	D_{max} (Gy)	64.01±7.80	67.22±8.68	0.116
	V_{45} (%)	30.75±10.06	87.26±19.37	0.028*

Abbreviations: Dmax: maximum dose; Dmean: mean dose; Dmin: minimum dose, D1cc and D10cc : dose covering 1 cm3 and 10 cm3 of PTV, respectively; Percentage of V5, V20, V45, V50, V55, V75: represent volumes of 5, 20, 50, 55, and 75 of PTV. *Statistically significant at the level of 5%. Errors are standard deviation; the last column shows the P-value between the two groups. * is a sign that the difference between the two groups is significant.

[DOI: 10.61186/ijrr.21.3.427]

DISCUSSION

One of the most important parameters of evaluating treatment plans is to cover the target volume of the case $V_{95\%}$, the percentage of the target volume that has received 95% of the prescribed dose. According to the obtained results, HT performed significantly better than 3D-CRT in terms of the target volume coverage. According to the CI definition, the ideal state of full PTV with the prescribed isodose curve in the treatment design or CI value is one. The closer the values of this index are to 1, the more valuable it will be. Conformity index values for the HT method are significantly closer to 1. The reason is a high dose gradient around target volumes, no limit on the number of treatment fields, the non-uniform intensity of radiation from different directions, application of dose-volume constraints to the treatment planning system, use of iteration-based computer algorithms to find the optimal solution, and application of parameters like Importance and Penalty to control the optimization process.

The homogeneity index is a ratio to assess PTV homogeneity. Larger HI values indicate weaker homogeneity in PTV. The closer this quantity is to zero, the more valuable it is. In the HT, the HI values for PTV and PTV Nodal were closer to zero. Therefore, homogeneous dose distribution was observed in HT, due to the application of dose constraints to target volumes and consequently reducing the volume of regions with doses of more than 107% and less than 95%.

In some cases, the target volumes overlapped with the adjacent OARs in the treatment planning. When sparing OARs is considered, it is more important than dose homogeneity and adequate PTV coverage.

The ICRU recommends that the absorbed dose in PTV be limited to between 95% and 107% of the prescribed dose. The extent of regions with high and low doses is determined using dose-volume values such as $D_{2\%}$ and $D_{98\%}$ for regions with high and low absorption doses, respectively. In HT, $D_{2\%}$ values for PTV and PTV Nodal were significantly reduced compared to 3D-CRT, and resulted in reduction hot spots or regions with a high absorbed dose in HT compared to 3D-CRT. The $D_{98\%}$ parameter in the HT increased compared to 3D-CRT, which means that in the HT, a decrease in cold spots or regions with a low absorption dose is encountered. Therefore, the HT method performed better than 3D-CRT in reducing hot and cold spots or regions with high and low absorbed doses. Consequently, reducing cold spots or regions with less than the required absorbed dose means reducing the possibility of tumor recurrence and reducing hot spots or regions with excessive absorbed dose reduces the complications and side effects after treatment.

According to results of table 7, most of the parameters compared between the critical structures showed a statistically significant difference between the two studied techniques ($P<0.005$), meaning that most of these structures received higher doses in the 3D-CRT compared to HT.

In a study [21], the dose received by the spinal cord for the 3D-CRT method was significantly lower than the HT method, which is not in agreement with results of this study. But, the dose received was much lower than the tolerance dose limit of the spinal cord and this increase in the dose for the spinal cord happened at the cost of a decrease in the dose for the carotids and thyroid, which causes less potential side effects for the patient.

In this study, unlike HT, 3D-CRT was not able to meet the mean dose range < 26 Gy for the parotids, and HT significantly reduced the mean dose received by the right and left parotids compared to 3D-CRT (table 7). In 2019, Teng *et al.* [22] reported a D_{mean} of 29.12 Gy for parotid in HT, which is higher than the D_{mean} obtained in this study.

The D_{max} of the oral cavity in Santa Cruz *et al.* [23] study with the HT method was 42±18 Gy which is lower than the value obtained in the present study (table 7). The D_{mean} of the oral cavity in a study conducted by Leung *et al.* [24] was 32.49±6.09 Gy in comparison to 41.08±7.02 Gy in the present work. The reason for the difference in these values could be related to the difference in tumor location in the two mentioned studies. The oral cavity is one of the parallel organs, the D_{mean} is more suitable and its value was slightly higher in 3D-CRT compared to HT.

In HT technique, the D_{max} of mandible in previous studies was 56±12 Gy (23) and 63.64±1.27 Gy [24] and 55.5±1.3 and 56.5±0.8 Gy [15]. In this study, it was 62.5±9.56 Gy, which is more than some studies and less than some others and meets the specified dose range. This value is significantly lower than the value obtained for the 3D-CRT method and for 3D-CRT is out of range.

The D_{mean} of larynx in Santa Cruz *et al.* [23] work was 29±13 Gy and in the present study it is less than the value obtained from the 3D-CRT method. The D_{max} of thyroid by HT in Santa Cruz *et al.* [23] study was 52±19 Gy, but it was higher in this study, which is still more than the prescribed dose range of previous study. In this study, this value was higher in the 3D-CRT method. Therefore, the HT method did not show much difference in thyroid protection compared to 3D-CRT. The D_{max} of brainstem in previous studies was 50.53±1.78 Gy [24] and 20±12 Gy [23] and 30.60±4.41 Gy in HT and it was 4.21±4.21 33.74 Gy in 3D-CRT (25). In this study, the D_{max} of brainstem was obtained 32.09±16.40 Gy in HT and 46.09±18.16 Gy in 3D-CRT.

Also, the D_{mean} of right and left cochlea with HT was reported as 6.5 and 6 Gy in Nguyen *et al.* [26] work and in this study these values are higher than the previous mentioned study, but they are still lower

[DOI: 10.61186/ijrr.21.3.427]

than the intended dose limit and significantly lower than the values obtained for the 3D-CRT method. The results of this work are in a good agreement with Myers *et al.* [27] study, which they have claimed that HT may provide patients with better long-term outcomes after radiotherapy.

The results in table 7, showed that 3D-CRT, in many cases, was not able to meet the desired constraints for OARs. This was especially evident in the case of serial structures such as the spinal cord, even despite prioritizing the spinal cord over target volumes in 3D-CRT. In most OARs, a decrease in the D_{mean} received in 3D-CRT compared to HT.

All of these findings and their comparison can confirm that HT is a more successful method in sparing oral cavity, mandible, larynx, cochlea, and brainstem.

Despite the potential advantages of the HT technique compared to 3D-CRT, it has superiority for cases with lymph nodes involvement in the head and neck region, due to the wideness and multiplicity of target volumes and numerous OARs, but sometimes their overlap with the target volumes has remained unclear.

CONCLUSION

In the present study, dosimetric characteristics of HT and 3D-CRT methos are assessed and compared based on the results of treatment planning for head and neck cancer patients with regional lymph node involvement. Findings showed significant improvements in sparing OARs such as spinal cord and parotids, reduction in the volume of cold and hot spots, and better dose coverage of target volumes for HT compared to 3D-CRT. The HT also performed significantly better than the 3D-CRT in the dose homogeneity and conformity indices that was not possible in 3D-CR. Overall, with the satisfactory results obtained HT technique has considerable promise to treatment head and neck cancer with the involvement of regional lymph nodes.

ACKNOWLEDGMENT

The authors would like to thank the staff of radiotherapy department of Seyed Al-shohada, Isfahan, Iran for their helpful guidance on various technical issues examined in this work.

***Financial support*:** This work financially was supported (grant no: 399018 and 199596) by the Isfahan University of Medical Sciences, Isfahan, Iran.

***Ethical approval*:** This work was done according to ethical code no: IR.MUI.MED.REC.1399.1129.

***Conflicts of interest*:** The authors declare that they have no conflicts of interest.

***Author contribution*:** Study conception and design: (D.Sh-G), (N.M), (A.A); Data collection: (N.M), (Sh.M), (L.M), (A.Sh). Analysis and interpretation of results: (D.Sh-G), (N.M), (R.M); Draft manuscript preparation: (N.M), (D.Sh-G), (Sh.M); Draft review and editing: (D.Sh-G); Supervision: (D.Sh-G), (A.A); Project Administration: (D.Sh-G); Funding Acquisition: (D.Sh-G).

REFERENCES

1. Ralston SH, Penman ID, Strachan MW, Hobson R (2022) Davidson's principles and practice of medicine. E-book: *Elsevier health sciences, 24th ed.,* ISBN: 9780702083495
2. Shang Q, Shen ZL, Ward MC, *et al.* (2015) Evolution of treatment planning techniques in external-beam radiation therapy for head and neck cancer. *Applied Radiation Oncology, **4**:18-25.*
3. Andrew DV, Gregory MM, Videtic NW (2014) Handbook of treatment planning. *2nd Ed., Springer Publishing Company, New York, United States.*
4. Moroney LB, Helios J, Ward EC, *et al.* (2017) Patterns of dysphagia and acute toxicities in patients with head and neck cancer undergoing helical IMRT±concurrent chemotherapy. *Oral Oncology, **64**:1-2.*
5. Low DA, Moran JM, Dempsey JF, *et al.* (2011) Dosimetry tools and techniques for IMRT. *Medical Physics, **38**(3):1313-38.*
6. Gupta T, Agarwal J, Jain S, *et al.* (2012) Three-dimensional conformal radiotherapy (3D-CRT) versus intensity modulated radiation therapy (IMRT) in squamous cell carcinoma of the head and neck: a randomized controlled trial. *Radiotherapy & Oncology,**104**(3): 343-8.*
7. Cheng HC, Wu VW, Ngan RK, *et al.* (2012) A prospective study on volumetric and dosimetric changes during intensity-modulated radiotherapy for nasopharyngeal carcinoma patients. *Radiotherapy & Oncology, **104**(3): 317-23.*
8. Teoh M, Clark C, Wood K, *et al.* (2011) Volumetric modulated arc therapy: a review of current literature and clinical use in practice. *The British Journal of Radiology, **84**(1007): 967-96.*
9. Bedford JL and Warrington AP (2009) Commissioning of volumetric modulated arc therapy (VMAT). *Int J Radiat Oncolo Biol Phys, **73**(2): 537-45.*
10. Buettner F, Miah AB, Gulliford SL, *et al.* (2012) Novel approaches to improve the therapeutic index of head and neck radiotherapy: an analysis of data from the PARSPORT randomised phase III trial. *Radiotherapy & Oncology, **103**(1): 82-7.*
11. Nutting CM, Morden JP, Harrington KJ, *et al.* (2011) Parotid-sparing intensity modulated versus conventional radiotherapy in head and neck cancer (PARSPORT): a phase 3 multicentre randomised controlled trial. *The Lancet Oncology, **12**(2): 127-36.*
12. Elith C, Dempsey SE, Findlay N, *et al.* (2011) An introduction to the intensity-modulated radiation therapy (IMRT) techniques, tomotherapy, and VMAT. *Journal of Medical Imaging & Radiation Sciences, **42**(1): 37-43.*
13. Jeraj R, Mackie TR, Balog J, *et al.* (2004) Radiation characteristics of helical tomotherapy. *Medical Physics, **31**(2): 396-404.*
14. Shen Q, Ma X, Hu W, *et al.* (2013) Intensity-modulated radiotherapy versus three-dimensional conformal radiotherapy for stage I-II natural killer/T-cell lymphoma nasal type: dosimetric and clinical results. *Radiation Oncology, **8**(1): 1-8.*
15. Fiorino C, Dell'Oca I, Pierelli A, *et al.* (2006) Significant improvement in normal tissue sparing and target coverage for head and neck cancer by means of helical tomotherapy. *Radiotherapy & Oncology, **78**(3): 276-82.*
16. Cao D, Holmes TW, *et al.* (2007) Comparison of plan quality provided by intensity-modulated arc therapy and helical tomotherapy. *In J Radiat Oncol Biol Phys, **69**(1):240-50.*
17. Murthy V, Master Z, Gupta T, *et al.* (2010) Helical tomotherapy for head and neck squamous cell carcinoma: dosimetric comparison with linear accelerator-based step-and-shoot IMRT. *Journal of Cancer Research & Therapeutics, **6**(2): 194.*
18. Rong Y, Tang G, Welsh JS, *et al.* (2011) Helical tomotherapy versus single-arc intensity-modulated arc therapy: a collaborative dosimetric comparison between two institutions. *Int J Radiat Oncol Biol Phy, **81**(1): 284-96.*
19. Wiezorek T, Brachwitz T, Georg D, *et al.* (2011) Rotational IMRT techniques compared to fixed gantry IMRT and tomotherapy: multi-institutional planning study for head-and-neck cases. *Radiation Oncology, **6**(1):1-10.*

[DOI: 10.61186/ijrr.21.3.427]

20. Grégoire V and Mackie TR (2011) Optimized Treatment Planning For IMRT, comparison of 3D-Conformal and IMRT treatment planning. *Cancer/Radiothérapie,* ***2011****:17-25.*
21. Ekici K, Pepele EK, Yaprak B, *et al.* (2016) Dosimetric comparison of helical tomotherapy, intensity-modulated radiation therapy, volumetric-modulated arc therapy, and 3-dimensional conformal therapy for the treatment of T1N0 glottic cancer. *Medical Dosimetry,* ***41****(4): 329-33.*
22. Teng F, Fan W, Luo Y, *et al.* (2019) Reducing xerostomia by comprehensive protection of salivary glands in intensity-modulated radiation therapy with helical tomotherapy technique for head-and-neck cancer patients: a prospective observational study. *BioMed Research International,* ***2019****:* 2401743.
23. Santa Cruz O, Tsoutsou P, Castella C, *et al.* (2018) Locoregional control and toxicity in head and neck carcinoma patients following helical Tomotherapy-delivered intensity-modulated radiation therapy compared with 3D-CRT data. *Oncology,* ***95****:61-8.*
24. Leung SW and Lee TF (2013) Treatment of nasopharyngeal carcinoma by tomotherapy: five-year experience. *Radiation Oncology,* ***8*** *(1): 1-6.*
25. Liu X, Huang E, Wang Y, *et al.* (2017) Dosimetric comparison of helical tomotherapy, VMAT, fixed-field IMRT and 3D-conformal radiotherapy for stage I-II nasal natural killer *T-cell* lymphoma. *Radiation Oncology, 12****(1)****:1-9.*
26. Nguyen NP, Smith-Raymond L, Vinh-Hung V, *et al.* (2011) Feasibility of Tomotherapy to spare the cochlea from excessive radiation in head and neck cancer. *Oral Oncology,* ***47****(5): 414-9.*
27. Myers PA, Mavroidis P, Papanikolaou N, Stathakis S (2014) Comparing conformal, arc radiotherapy and helical tomotherapy in craniospinal irradiation planning. *Journal of Applied Clinical Medical Physics,* ***15****(5):4724.*

[DOI: 10.61186/ijrr.21.3.427]